Available online at http://scik.org
Commun. Math. Biol. Neurosci. 2025, 2025:34
https://doi.org/10.28919/cmbn/9147
ISSN: 2052-2541

STABILITY AND BIFURCATION ANALYSIS OF A DISCRETE FRACTIONAL ORDER PREDATOR-PREY LESLIE-GOWER MODEL WITH FEAR EFFECT, ALLEE EFFECT, AND INTERSPECIES RIVALRY

SRI PUJI LESTARI, AGUS SURYANTO*, ISNANI DARTI

Department of Mathematics, Faculty of Mathematics and Natural Sciences,
University of Brawijaya, Malang 65145, Indonesia

Abstract. This paper discusses the analysis of a discrete fractional-order Leslie-Gower model with fear effects, Allee effects, and interspecies competition. The discrete model is obtained by discretizing the continuous model using the piecewise constant approximation method. The model has four fixed points, namely trivial fixed point, prey extinction fixed point, predator extinction fixed point, and interior fixed point. The trivial fixed point always exists, while the existence of prey extinction, predator extinction, and interior fixed points are determined by certain conditions. The stability analysis shows that there are topological differences that depend on the parameter and the size of the integration step. Bifurcation analysis is performed using center manifold theory and bifurcation theorem. By choosing the integration step as the bifurcation parameter, it can be shown that the model experiences period-doubling bifurcation and Neimark-Sacker bifurcation. Numerical simulations are carried out at the end of this paper to confirm the analytical results.

Keywords: fear effect; Allee effect; period-doubling bifurcation; Neimark-Sacker bifurcation.

2020 AMS Subject Classification: 39A28, 39A39, 92D25, 92D40.

1. INTRODUCTION

Every organism will always interact with other organisms or the environment around them. The interaction between a population and other populations affects the ecological system [1].

---

*Corresponding author
E-mail address: suryanto@ub.ac.id
Received January 23, 2025

According to Mader [2], one example of interaction between two populations that occurs due to the relationship of eating and being eaten between predator and prey is predation. Mathematical models can be used to describe interactions between predator and prey, such as [3, 4, 5, 6].

Phenomena in populations are very diverse, one of which is the Allee Effect. The Allee effect is the positive dependence of a population on the number of individuals. If the population is too small, finding partners to reproduce will be more difficult, resulting in low birth rates. In addition, food supplies for predators will decrease, resulting in higher death rates for predators [7, 8, 9, 10, 11, 12].

Interactions between predator and prey populations can be divided into two types, namely direct and indirect interactions. Direct interactions can be in the form of predation [13], while indirect interactions can be in the form of predator populations that cause fear in prey and impact changes in prey behavior [14]. Prey avoids direct predation to increase prey survival in the short term but threatens the number of prey in the long term [15]. Compared with direct predation, these fear-induced behavioral changes can have stronger and longer-lasting effects [16, 17]. Other studies on the effects of fear are [18, 19, 20, 21, 22].

Depending on current and previous conditions, the rate of change in predator-prey populations can be modeled as a fractional order differential equations system. Fractional differential equations are used in various fields, such as biology, fluid dynamics, medicine, and others [23]. Several researchers such as [24, 25, 26, 27] use fractional order in the model because fractional differential equations are found to use memory so that this equation has a more realistic relationship with life. The memory effect in the predator-prey model is important because previous memories can be embedded in the lives of predators and prey [28, 29, 30]. In [31, 32], fear affects local stability and causes Hopf bifurcation in the system.

Furthermore, combining Allee effects and fear effects in fractional order models is interesting to study. This combination has been studied by Kumar et al. [32] in the following fractional order of continuous Leslie-Gower predator-prey model with Allee effect, fear effect, and interspecies rivalry.

$$
\begin{aligned}
{}^{C}D_t^{\alpha} u &= \frac{ru}{1+\theta_0 v} - pu - qu^2 - \frac{muv}{u+kv}, \\
{}^{C}D_t^{\alpha} v &= bv\left(\frac{v}{v+\theta_1} - \frac{v}{cu+d}\right),
\end{aligned} \tag{1.1}
$$

where $u(t)$ and $v(t)$ represent the population density of prey and predators at time t respectively. The parameter α, h, r, m, k, θ_0, p, q, b, c, d, θ_1 are fractional order, step size, prey intrinsic birth rate, predation rate, prey handling time, fear effect, prey natural mortality rate, inter-prey competition rate, predator intrinsic birth rate, carrying capacity for predators, food supply level for predators, and Allee effect.

The exact solution to the model in a nonlinear differential equation (1.1) is difficult to determine analytically, so a numerical scheme is needed that changes the continuous model to a discrete one. According to Podlubny [33], one of the numerical approximation methods used to discretize fractional differential equations is the PWCA (Piecewise Constant Approximation) method. This method is applied by dividing a continuous interval into some subintervals and assuming that the constant function in each subinterval [34, 35, 36, 37, 38]. By applying the PWCA method to system (1.1), we obtain

$$
\begin{aligned}
u_{n+1} &= u_n + \frac{h^\alpha}{\alpha\Gamma(\alpha)}\left(\frac{ru_n}{1+\theta_0 v_n} - pu_n - qu_n^2 - \frac{mu_n v_n}{u_n + kv_n}\right), \\
v_{n+1} &= v_n + \frac{h^\alpha}{\alpha\Gamma(\alpha)}\left(bv_n\left(\frac{v_n}{v_n+\theta_1} - \frac{v_n}{cu_n+d}\right)\right),
\end{aligned} \tag{1.2}
$$

where $u_n = u(t_n)$, $v_n = v(t_n)$ and $h = \Delta t$ is the step size of the numerical integration. The obtained discrete model is consistent with the continuous model if it maintains dynamic properties, such as fixed points, stability, oscillations, etc. [39]. On the other hand, discrete models can produce more complex and interesting dynamic behavior than continuous models [40, 41, 38].

Based on the previous description, in this paper, we carry out the dynamical analysis for the system (1.2). This analysis includes determining the existence and stability of fixed points in Section 2, bifurcation analysis in Section 3, and numerical simulation in Section 4. Lastly, in Section 5, we give a conclusion of our findings.

2. The Existence and Stability of Fixed Points

System (1.2) has four types of positive fixed points, namely the trivial fixed point $E_0(0,0)$ which always exists, the predator extinction fixed point $E_1\left(\frac{r-p}{q},0\right)$ which exists if $r > p$, the prey extinction fixed point $E_2(0,d-\theta_1)$ which exists if $d > \theta_1$, and the interior fixed point $E^*(u^*,v^*)$, where $u^* = \frac{v^*+\theta_1-d}{c}$ and v^* satisfy the following cubic equation

$$v^{*3} + 3v^{*2}\rho_1 + 3v^*\rho_2 + \rho_3 = 0,$$

with

$$\rho_1 = \frac{q\theta_0(ck+2)(\theta_1 - d) + (ck+1)(cp\theta_0 + q) + \theta_0 c^2 m}{3q\theta_0(ck+1)},$$
$$\rho_2 = \frac{mc^2 + q\theta_0(\theta_1 - d)^2 + (ckq + cp\theta_0 + 2q)(\theta_1 - d) + c(ck+1)(p-r)}{3q\theta_0(ck+1)},$$
$$\rho_3 = \frac{q(\theta_1 - d)^2 + c(\theta_1 - d)(p-r)}{q\theta_0(ck+1)}.$$

$E^*(u^*, v^*)$ exists if both u^* and v^* are positive, which can be determined by applying Cardan's method as [42, Lemma 3.1]. The Jacobian matrix of (1.2) at a fixed point $(\hat{u}, \hat{v})$ is

$$J = \begin{bmatrix} j_{11} & j_{12} \\ j_{21} & j_{22} \end{bmatrix}, \tag{2.1}$$

where $j_{11} = 1 + \frac{h^\alpha}{\alpha\Gamma(\alpha)}\left(-q\hat{u} + \frac{m\hat{u}\hat{v}}{(\hat{u}+k\hat{v})^2}\right)$, $j_{12} = \frac{h^\alpha}{\alpha\Gamma(\alpha)}\left(-\frac{r\hat{u}\theta_0}{(1+\theta_0\hat{v})^2} - \frac{m\hat{u}^2}{(\hat{u}+k\hat{v})^2}\right)$, $j_{21} = \frac{h^\alpha}{\alpha\Gamma(\alpha)}\frac{b\hat{v}^2 c}{(c\hat{u}+d)^2}$, and $j_{22} = 1 - \frac{h^\alpha}{\alpha\Gamma(\alpha)}\frac{b\hat{v}^2}{(\hat{v}+\theta_1)^2}$. The characteristic equation of the Jacobian matrix is given by

$$F(\lambda) = \lambda^2 - (2 + \eta_a\zeta_a)\lambda + (1 + \eta_a\zeta_a + \eta_a^2\omega_a) = 0, \tag{2.2}$$

where

$$\eta_a = \frac{h^\alpha}{\alpha\Gamma(\alpha)},$$
$$\zeta_a = -q\hat{u} + \frac{m\hat{u}\hat{v}}{(\hat{u}+k\hat{v})^2} - \frac{b\hat{v}^2}{(\hat{v}+\theta_1)^2},$$
$$\omega_a = -\frac{b\hat{v}^2}{(\hat{v}+\theta_1)^2}\left(-q\hat{u} + \frac{m\hat{u}\hat{v}}{(\hat{u}+k\hat{v})^2}\right) + \frac{b\hat{v}^2 c}{(c\hat{u}+d)^2}\left(\frac{r\hat{u}\theta_0}{(1+\theta_0\hat{v})^2} + \frac{m\hat{u}^2}{(\hat{u}+k\hat{v})^2}\right).$$

The local stability of fixed points is given in the following theorem.

Theorem 2.1. *The trivial fixed point $E_0(0,0)$ is a non-hyperbolic point.*

Proof. By substituting E_0 into (2.1), it can be shown that $J(E_0)$ has eigenvalues $\lambda_1 = 1 + \frac{h^\alpha}{\alpha\Gamma(\alpha)}(r-p)$ and $\lambda_2 = 1$. Thus, E_0 is a non-hyperbolic point. □

Theorem 2.2. *The predator extinction fixed point $E_1 = \left(\frac{r-p}{q}, 0\right)$ is a non-hyperbolic point.*

Proof. By evaluating E_1 into (2.1), $J(E_1)$ has eigenvalues $\lambda_1 = 1 + \frac{h^\alpha}{\alpha\Gamma(\alpha)}(p-r)$ and $\lambda_2 = 1$. Hence, E_1 is a non-hyperbolic point. □

Theorem 2.3. *Let $G = \frac{r}{1+\theta_0(d-\theta_1)} - p - \frac{m}{k}$, $H_1 = \sqrt[\alpha]{\frac{-2\alpha\Gamma(\alpha)}{G}}$, and $H_2 = \sqrt[\alpha]{\frac{2d^2\alpha\Gamma(\alpha)}{b(d-\theta_1)^2}}$. The prey extinction fixed point $E_2(0, d-\theta_1)$ has the following properties.*

(1) E_2 is a sink if $h < \min\{H_1, H_2\}$ and $G < 0$.

(2) E_2 is a source if one of the following conditions satisfies:

(a) $h > \max\{H_1, H_2\}$ and $G < 0$;

(b) $h > H_2$ and $G > 0$.

(3) E_2 is a saddle if one of the following conditions holds:

(a) $H_1 < h < H_2$ and $G < 0$;

(b) $0 < h < H_2$ and $G > 0$.

(4) E_2 is a non-hyperbolic if one of the following conditions holds:

(a) $G = 0$ or $h = H_1$;

(b) $h = H_2$.

Proof. By evaluating E_2 into (2.1), we get $\lambda_1 = 1 + \frac{h^\alpha}{\alpha\Gamma(\alpha)}\left(\frac{r}{1+\theta_0(d-\theta_1)} - p - \frac{m}{k}\right)$ and $\lambda_2 = 1 + \frac{h^\alpha}{\alpha\Gamma(\alpha)}\left(-\frac{b(d-\theta_1)^2}{d^2}\right)$. In this case, we obtain $|\lambda_1| < 1$ if $0 < h < H_1$ and $G < 0$. $|\lambda_1| > 1$ if $h > H_1$ and $G < 0$, or $G > 0$. $|\lambda_1| = 1$ if $G = 0$ or $h = H_1$. Furthermore, $|\lambda_2| < 1$ if $0 < h < H_2$, $\lambda_2 > 1$ if $h > H_2$. $|\lambda_2| = 1$ if $h = H_2$. □

Based on equation (2.2), we obtain $F(1) = \omega_a$, $F(0) = 1 + \eta_a\zeta_a + \eta_a^2\omega_a$, and $F(-1) = 4 + 2\eta_a\zeta_a + \eta_a^2\omega_a$. By using the stability criterion in [43] and the properties of quadratic equation for (2.2) in [21, Lemma 1-2], the following properties hold.

Theorem 2.4. *Let $\eta_{a_{1,2}} = \frac{-\zeta_a \mp \sqrt{\zeta_a^2 - 4\omega_a}}{\omega_a}$ which is equivalent to $h_{1,2} = \left(\frac{-\zeta_a \mp \sqrt{\zeta_a^2 - 4\omega_a}}{\omega_a}\Gamma(1+\alpha)\right)^{\frac{1}{\alpha}}$. If the coexistence fixed point $E^*(u^*, v^*)$ exists, the properties of $E^*(u^*, v^*)$ are described based on the value of $F(1)$ as follows.*

(1) For $F(1) > 0$, the coexistence fixed point $E^*(u^*, v^*)$ has the following properties.

(a) E^* is a sink if one of the following conditions holds:

(i) $\zeta_a^2 - 4\omega_a > 0$ and $0 < \eta_a < \eta_{a_1}$;

  (ii) $\zeta_a^2 - 4\omega_a \le 0$ *and* $0 < \eta_a < -\frac{\zeta_a}{\omega_a}$.

 (b) E^* *is a source if one of the subsequent conditions holds:*

  (i) $\zeta_a^2 - 4\omega_a > 0$ *and* $\eta_a > \eta_{a_2}$*;*

  (ii) $\zeta_a^2 - 4\omega_a \le 0$ *and* $\eta_a > -\frac{\zeta_a}{\omega_a}$.

 (c) E^* *is a saddle if* $\zeta_a^2 - 4\omega_a > 0$ *and* $\eta_{a_1} < \eta_a < \eta_{a_2}$.

 (d) E^* *is a non-hyperbolic if one of the conditions below satisfies:*

  (i) $\zeta_a^2 - 4\omega_a > 0$ *and* $\eta_a = \eta_{a_{1,2}}$*;*

  (ii) $\zeta_a^2 - 4\omega_a \le 0$ *and* $\eta_a = -\frac{\zeta_a}{\omega_a}$.

(2) If $F(1) < 0$*, the coexistence fixed point* $E^*(u^*, v^*)$ *has the following properties.*

 (a) E^* *is a source if* $\eta_a > \eta_{a_2}$.

 (b) E^* *is a saddle if* $0 < \eta_a < \eta_{a_2}$.

 (c) E^* *is a non-hyperbolic if* $\eta_a = \eta_{a_2}$.

Proof. The proof is divided into the following two cases.

(1) Case $F(1) > 0$.

 (a) If $\zeta_a^2 - 4\omega_a > 0$, then $F(-1) = 0$ has two distinct real roots: $\eta_a = \eta_{a_{1,2}}$ and it follows that

  (i) if $0 < \eta_a < \eta_{a_1}$, then $|\lambda_1| < 1$ and $|\lambda_2| < 1$;

  (ii) if $\eta_a > \eta_{a_2}$, then $|\lambda_1| > 1$ and $|\lambda_2| > 1$;

  (iii) if $\eta_a = \eta_{a_1}$ or $\eta_a = \eta_{a_2}$, then $\lambda_1 = -1$ and $|\lambda_2| \ne 1$;

  (iv) if $\eta_{a_1} < \eta_a < \eta_{a_2}$, then $|\lambda_1| > 1$ and $|\lambda_2| < 1$ (or $|\lambda_1| < 1$ and $|\lambda_2| > 1$).

 (b) If $\zeta_a^2 - 4\omega_a = 0$, then $\eta_{a_{1,2}} = -\frac{\zeta_a}{\omega_a}$ and we have

  (i) if $0 < \eta_a < -\frac{\zeta_a}{\omega_a}$, then $|\lambda_1| < 1$ and $|\lambda_2| < 1$;

  (ii) if $\eta_a > -\frac{\zeta_a}{\omega_a}$, so $|\lambda_1| > 1$ and $|\lambda_2| > 1$;

  (iii) if $\eta_a = -\frac{\zeta_a}{\omega_a}$, then $\lambda_1 = \lambda_2 = 1$.

 (c) If $\zeta_a^2 - 4\omega_a < 0$, then $\eta_{a_{1,2}}$ are conjugate complex roots of $F(-1)$ and we obtain

  (i) if $0 < \eta_a < -\frac{\zeta_a}{\omega_a}$, then $|\lambda_1| < 1$ and $|\lambda_2| < 1$;

  (ii) if $\eta_a > -\frac{\zeta_a}{\omega_a}$, then $|\lambda_1| > 1$ and $|\lambda_2| > 1$;

  (iii) if $\eta_a = -\frac{\zeta_a}{\omega_a}$, then $|\lambda_1| = |\lambda_2| = 1$.

(2) Case $F(1) < 0$. In this case, $F(-1) < 0$ if $\eta_a < \eta_{a_1}$ or $\eta_a > \eta_{a_2}$, while $F(-1) > 0$ if $\eta_{a_1} < \eta_a < \eta_{a_2}$. So, we get the following properties.
   (a) If $\eta_a > \eta_{a_2}$, then $|\lambda_1| > 1$ and $|\lambda_2| > 1$.
   (b) If $0 < \eta_a < \eta_{a_2}$, then $|\lambda_1| < 1$ and $|\lambda_2| > 1$ (or $|\lambda_1| > 1$ and $|\lambda_2| < 1$).
   (c) If $\eta_a = \eta_{a_2}$, then $\lambda_1 = -1$ and $|\lambda_2| \neq 1$.

□

Based on the stability analysis, one of the eigenvalues of the Jacobian matrix around $E^*(u^*, v^*)$ is 1, and the other eigenvalue is neither 1 nor -1 if

$$P_{1,2} = \left\{ (\alpha, r, \theta_0, p, q, m, k, b, \theta_1, c, d, h) : \zeta_a^2 - 4\omega_a > 0, \eta_{a_{1,2}} = \frac{-\zeta_a \mp \sqrt{\zeta_a^2 - 4\omega_a}}{\omega_a} \right\},$$

where $\eta_{a_{1,2}}$ are equivalent to $h = \left(\frac{-\zeta_a \mp \sqrt{\zeta_a^2 - 4\omega_a}}{\omega_a} \Gamma(1+\alpha) \right)^{\frac{1}{\alpha}} = h_{1,2}$. Therefore, if the parameters vary around $P_{1,2}(E^*)$, a period-doubling bifurcation occurs on E^*. Besides, if

$$N = \left\{ (\alpha, r, \theta_0, p, q, m, k, b, \theta_1, c, d, h) : \zeta_a^2 - 4\omega_a < 0, \eta_a^* = -\frac{\zeta_a}{\omega_a} \right\},$$

where η_a^* is equivalent to $h = \left(-\frac{\zeta_a}{\omega_a} \Gamma(1+\alpha) \right)^{\frac{1}{\alpha}} = h^*$, then the eigenvalues of the Jacobian matrix at E^* are a pair of complex numbers with modulus 1. Thus, if the parameters vary around $N(E^*)$, the Neimark-Sacker bifurcation occurs at E^*.

3. Bifurcation Analysis

3.1. Period-doubling bifurcation. In this Section we discuss the period-doubling bifurcation analysis around the interior fixed point $E^*(u^*, v^*)$. Consider system (1.2) with any parameters $(\alpha, r, \theta_0, p, q, m, k, b, \theta_1, c, d, h) \in P_1$. Based on Theorem 2.4, $E^*(u^*, v^*)$ has eigen values, which are $\lambda_1 = -1$ and $\lambda_2 = 3 + \zeta_a \eta_{a1}$, where $|\lambda_2| \neq 1$. By introducing a small perturbation $\widetilde{\eta_a}, |\widetilde{\eta_a}| \ll 1$ into the system (1.2) around $\eta_a = \eta_{a_1}$, we get

$$(3.1) \qquad \begin{aligned} u_{n+1} &= u_n + (\eta_{a_1} + \widetilde{\eta_a}) \left(\frac{r u_n}{1 + \theta_0 v_n} - p u_n - q u_n^2 - \frac{m u_n v_n}{u_n + k v_n} \right), \\ v_{n+1} &= v_n + (\eta_{a_1} + \widetilde{\eta_a}) \left(b v_n \left(\frac{v_n}{v_n + \theta_1} - \frac{v_n}{c u_n + d} \right) \right). \end{aligned}$$

Then, we shift the fixed point $E^*(u^*,v^*)$ to the origin using transformations $x_n = u_n - u^*$ and $y_n = v_n - v^*$, so that the system (3.1) becomes

(3.2)
$$\begin{aligned}
x_{n+1} =& \sigma_{11}x_n + \sigma_{12}y_n + \sigma_{13}x_n^2 + \sigma_{14}x_ny_n + \sigma_{15}y_n^2 + \sigma_{16}x_n^3 + \sigma_{17}x_n^2y_n + \sigma_{18}x_ny_n^2 + \sigma_{19}y_n^3 \\
&+ \varsigma_{11}x_n\widetilde{\eta_a} + \varsigma_{12}y_n\widetilde{\eta_a} + \varsigma_{13}x_n^2\widetilde{\eta_a} + \varsigma_{14}x_ny_n\widetilde{\eta_a} + \varsigma_{15}y_n^2\widetilde{\eta_a} + O((|x_n| + |y_n| + |\widetilde{\eta_a}|)^4), \\
y_{n+1} =& \sigma_{21}x_n + \sigma_{22}y_n + \sigma_{23}x_n^2 + \sigma_{24}x_ny_n + \sigma_{25}y_n^2 + \sigma_{26}x_n^3 + \sigma_{27}x_n^2y_n + \sigma_{28}x_ny_n^2 + \sigma_{29}y_n^3 \\
&+ \varsigma_{21}x_n\widetilde{\eta_a} + \varsigma_{22}y_n\widetilde{\eta_a} + \varsigma_{23}x_n^2\widetilde{\eta_a} + \varsigma_{24}x_ny_n\widetilde{\eta_a} + \varsigma_{25}y_n^2\widetilde{\eta_a} + O((|x_n| + |y_n| + |\widetilde{\eta_a}|)^4),
\end{aligned}$$

where

(3.3)
$$\begin{aligned}
&\sigma_{11} = 1 + \eta_{a_1}\left(-qu^* + \frac{mu^*v^*}{(u^*+kv^*)^2}\right), \quad \sigma_{12} = \eta_{a_1}\left(-\frac{ru^*\theta_0}{(1+\theta_0v^*)^2} - \frac{mu^{*^2}}{(u^*+kv^*)^2}\right), \\
&\sigma_{13} = \eta_{a_1}\left(-q + \frac{mkv^{*^2}}{(u^*+kv^*)^3}\right), \quad \sigma_{14} = \eta_{a_1}\left(-\frac{r\theta_0}{(1+\theta_0v^*)^2} - \frac{2mku^*v^*}{(u^*+kv^*)^3}\right), \\
&\sigma_{15} = \eta_{a_1}\left(\frac{ru^*\theta_0^2}{(1+\theta_0v^*)^3} + \frac{mu^{*^2}k}{(u^*+kv^*)^3}\right), \quad \sigma_{16} = -\eta_{a_1}\frac{mkv^{*^2}}{(u^*+kv^*)^3}, \\
&\sigma_{17} = \eta_{a_1}\left(\frac{2mku^*v^* - mk^2v^{*^2}}{(u^*+kv^*)^4}\right), \quad \sigma_{18} = \eta_{a_1}\left(\frac{r\theta_0^2}{(1+\theta_0v^*)^3} + \frac{2mk^2u^*v^* - mku^{*^2}}{(u^*+kv^*)^4}\right), \\
&\sigma_{19} = \eta_{a_1}\left(-\frac{ru^*\theta_0^3}{(1+\theta_0v^*)^4} - \frac{mk^2u^{*^2}}{(u^*+kv^*)^4}\right), \quad \varsigma_{11} = -qu^* + \frac{mu^*v^*}{(u^*+kv^*)^2}, \\
&\varsigma_{12} = -\frac{ru^*\theta_0}{(1+\theta_0v^*)^2} - \frac{mu^{*^2}}{(u^*+kv^*)^2}, \quad \varsigma_{13} = -q + \frac{mkv^{*^2}}{(u^*+kv^*)^3}, \\
&\varsigma_{14} = -\frac{r\theta_0}{(1+\theta_0v^*)^2} - \frac{2mku^*v^*}{(u^*+kv^*)}, \quad \varsigma_{15} = \frac{ru^*\theta_0^2}{(1+\theta_0v^*)^3} + \frac{mu^{*^2}k}{(u^*+kv^*)^3}, \\
&\sigma_{21} = \eta_{a_1}\frac{bv^{*^2}c}{(cu^*+d)^2}, \quad \sigma_{22} = 1 + \eta_{a_1}\left(\frac{2bv^*\theta_1 + bv^{*^2}}{(v^*+\theta_1)^2} - \frac{2bv^*}{cu^*+d}\right), \\
&\sigma_{23} = -\eta_{a_1}\frac{bv^{*^2}c^2}{(cu^*+d)^3}, \quad \sigma_{24} = \eta_{a_1}\frac{2bv^*c}{(cu^*+d)^2}, \quad \sigma_{25} = \eta_{a_1}\left(\frac{b\theta_1^2}{(\theta_1+v^*)^3} - \frac{b}{cu^*+d}\right), \\
&\sigma_{26} = \eta_{a_1}\frac{bv^{*^2}c^3}{(cu^*+d)^4}, \quad \sigma_{27} = -\eta_{a_1}\frac{2bv^*c^2}{(cu^*+d)^3}, \quad \sigma_{28} = \eta_{a_1}\frac{bc}{(cu^*+d)^2}, \\
&\sigma_{29} = -\eta_{a_1}\frac{b\theta_1^2}{(\theta_1+v^*)^4}, \quad \varsigma_{21} = \frac{bv^{*^2}c}{(cu^*+d)^2}, \quad \varsigma_{22} = \frac{2bv^*\theta_1 + bv^{*^2}}{(v^*+\theta_1)^2} - \frac{2bv^*}{cu^*+d}, \\
&\varsigma_{23} = -\frac{bv^{*^2}c^2}{(cu^*+d)^3}, \quad \varsigma_{24} = \frac{2bv^*c}{(cu^*+d)^2}, \quad \varsigma_{25} = \frac{b\theta_1^2}{(\theta_1+v^*)^3} - \frac{b}{cu^*+d}.
\end{aligned}$$

Next, we take the transformation $\begin{bmatrix} x_n \\ y_n \end{bmatrix} = T_1 \begin{bmatrix} U_n \\ V_n \end{bmatrix}$, where $T_1 = \begin{bmatrix} \sigma_{12} & \sigma_{12} \\ -1-\sigma_{11} & \lambda_2-\sigma_{11} \end{bmatrix}$, such that system (3.2) can be written as

$$\begin{bmatrix} U_{n+1} \\ V_{n+1} \end{bmatrix} = \begin{bmatrix} -1 & 0 \\ 0 & \lambda_2 \end{bmatrix} \begin{bmatrix} U_n \\ V_n \end{bmatrix} + \begin{bmatrix} \tilde{f}(U_n,V_n,\widetilde{\eta_a}) \\ \tilde{g}(U_n,V_n,\widetilde{\eta_a}) \end{bmatrix}, \tag{3.4}$$

where

$$\begin{aligned}
\tilde{f}(U_n,V_n,\widetilde{\eta_a}) =& \frac{1}{\sigma_{12}(\lambda_2+1)}\{[(\lambda_2-\sigma_{11})\sigma_{13}-\sigma_{12}\sigma_{23}]x_n^2 \\
&+[(\lambda_2-\sigma_{11})\sigma_{14}-\sigma_{12}\sigma_{24}]x_ny_n+[(\lambda_2-\sigma_{11})\sigma_{15}-\sigma_{12}\sigma_{25}]y_n^2 \\
&+[(\lambda_2-\sigma_{11})\sigma_{16}-\sigma_{12}\sigma_{26}]x_n^3+[(\lambda_2-\sigma_{11})\sigma_{17}-\sigma_{12}\sigma_{27}]x_n^2v_n \\
&+[(\lambda_2-\sigma_{11})\sigma_{18}-\sigma_{12}\sigma_{28}]x_ny_n^2+[(\lambda_2-\sigma_{11})\sigma_{19}-\sigma_{12}\sigma_{29}]y_n^3 \\
&+[(\lambda_2-\sigma_{11})\varsigma_{11}-\sigma_{12}\varsigma_{21}]x_n\widetilde{\eta_a}+[(\lambda_2-a_{11})\varsigma_{12}-\sigma_{12}\varsigma_{22}]y_n\widetilde{\eta_a} \\
&+[(\lambda_2-\sigma_{11})\varsigma_{13}-\sigma_{12}\varsigma_{23}]x_n^2\widetilde{\eta_a}+[(\lambda_2-a_{11})\varsigma_{14}-\sigma_{12}\varsigma_{24}]x_ny_n\widetilde{\eta_a} \\
&+[(\lambda_2-\sigma_{11})\varsigma_{15}-\sigma_{12}\varsigma_{25}]y_n^2\widetilde{\eta_a}+O((|x_n|+|y_n|+|\widetilde{\eta_a}|)^4)\}, \\
\tilde{g}(U_n,V_n,\tilde{h}) =& \frac{1}{\sigma_{12}(\lambda_2+1)}\{[(\sigma_{11}+1)\sigma_{13}+\sigma_{12}\sigma_{23}]x_n^2 \\
&+[(\sigma_{11}+1)\sigma_{14}+\sigma_{12}\sigma_{24}]x_ny_n+[(\sigma_{11}+1)\sigma_{15}+\sigma_{12}\sigma_{25}]y_n^2 \\
&+[(\sigma_{11}+1)\sigma_{16}+\sigma_{12}\sigma_{26}]x_n^3+[(\sigma_{11}+1)\sigma_{17}+\sigma_{12}\sigma_{27}]x_n^2y_n \\
&+[(\sigma_{11}+1)\sigma_{18}+\sigma_{12}\sigma_{28}]x_ny_n^2+[(\sigma_{11}+1)\sigma_{19}+\sigma_{12}\sigma_{29}]y_n^3 \\
&+[(\sigma_{11}+1)\varsigma_{11}+\sigma_{12}\varsigma_{21}]x_n\widetilde{\eta_a}+[(\sigma_{11}+1)\varsigma_{12}+\sigma_{12}\varsigma_{22}]y_n\widetilde{\eta_a} \\
&+[(\sigma_{11}+1)\varsigma_{13}+\sigma_{12}\varsigma_{23}]x_n^2\widetilde{\eta_a}+[(\sigma_{11}+1)\varsigma_{14}+\sigma_{12}\varsigma_{24}]x_ny_n\widetilde{\eta_a} \\
&+[(\sigma_{11}+1)\varsigma_{15}+\sigma_{12}\varsigma_{25}]y_n^2\widetilde{\eta_a}+O((|x_n|+|y_n|+|\widetilde{\eta_a}|)^4)\},
\end{aligned}$$

$x_n = \sigma_{12}(U_n+V_n)$ and $y_n = -(1+\sigma_{11})U_n+(\lambda_2-\sigma_{11})V_n$. Applying the center manifold theorem to system (3.4) at the origin near $\tilde{h}=0$, we obtain the following center manifold $W^c(0,0)$

$$W^c(0,0) = \{(U_n,V_n,\widetilde{\eta_a}) \in \mathbb{R}^3 : V_n = \varphi(U_n,\widetilde{\eta_a}), \varphi(0,0)=0, D\varphi(0,0)=0\},$$

where

$$\varphi(U_n,\widetilde{\eta_a})=\sigma_1U_n^2+\sigma_2U_n\widetilde{\eta_a}+\sigma_3\widetilde{\eta_a}+O((|U_n|+|\widetilde{\eta_a}|)^3).$$

The center manifold must satisfy

$$\begin{aligned}&[\sigma_1-\sigma_1\lambda_2-\frac{1}{\sigma_{12}(\lambda_2+1)}\{\sigma_{12}^2[(\sigma_{11}+1)\sigma_{13}+\sigma_{12}\sigma_{23}]-\sigma_{12}(\sigma_{11}+1)[(\sigma_{11}+1)\sigma_{14}+\sigma_{12}\sigma_{24}]\\&+(\sigma_{11}+1)^2[(\sigma_{11}+1)\sigma_{15}+\sigma_{12}\sigma_{25}]\}]u_n^2+[-\sigma_2-\sigma_2\lambda_2-\frac{1}{\sigma_{12}(\lambda_2+1)}\{\sigma_{12}[(\sigma_{11}+1)\varsigma_{11}+\sigma_{12}\varsigma_{21}]\\&-(\sigma_{11}+1)[(\sigma_{11}+1)\sigma_{12}+\sigma_{12}\varsigma_{22}]\}]u_n\widetilde{\eta_a}+(\sigma_3-\sigma_3\lambda_2)\widetilde{\eta_a}^2+O((|u_n|+|\widetilde{\eta_a}|)^3)=0.\end{aligned}$$

In the confined center manifold $W^c(0,0)$, system (3.4) can be expressed as

$$\tilde{\mathscr{F}}:U_n\mapsto -U_n+\phi_1U_n^2+\phi_2U_n\widetilde{\eta_a}+\phi_3U_n^2\widetilde{\eta_a}+\phi_4U_n\widetilde{\eta_a}^2+\phi_5U_n^3+O((|U_n|+|\widetilde{\eta_a}|)^3),$$

where

$$\begin{aligned}\phi_1=&\frac{1}{\sigma_{12}(\lambda_2+1)}\{\sigma_{12}^2[(\lambda_2-\sigma_{11})\sigma_{13}-\sigma_{12}\sigma_{23}]-\sigma_{12}(\sigma_{11}+1)[(\lambda_2-\sigma_{11})\sigma_{14}-\sigma_{12}\sigma_{24}]\\&+(\sigma_{11}+1)^2[(\lambda_2-\sigma_{11})\sigma_{15}-\sigma_{12}\sigma_{25}]\},\\ \phi_2=&\frac{1}{\sigma_{12}(\lambda_2+1)}\{\sigma_{12}[(\lambda_2-\sigma_{11})\varsigma_{11}-\sigma_{12}\varsigma_{21}]-(\sigma_{11}+1)[(\lambda_2-\sigma_{11})\varsigma_{12}-\sigma_{12}\varsigma_{22}]\},\\ \phi_3=&\frac{\sigma_2}{\sigma_{12}(\lambda_2+1)}\{2\sigma_{12}^2[(\lambda_2-\sigma_{11}\sigma_{13}-\sigma_{12}\sigma_{23})]+\sigma_{12}(\lambda_2-2\sigma_{11}-1)[(\lambda_2-\sigma_{11})\sigma_{14}-\sigma_{12}\sigma_{24}]\\&-2(\sigma_{11}+1)(\lambda_2-\sigma_{11})[(\lambda_2-\sigma_{11})\sigma_{15}-\sigma_{12}\sigma_{25}]\}+\frac{\sigma_1}{\sigma_{12}(\lambda_2+1)}\{\sigma_{12}[(\lambda_2-\sigma_{11})\varsigma_{11}-\sigma_{12}\varsigma_{21}]\\&+(\lambda_2-\sigma_{11})[(\lambda_2-\sigma_{11})\varsigma_{12}-\sigma_{12}\varsigma_{22}]\}+\frac{1}{\sigma_{12}(\lambda_2+1)}\{\sigma_{12}^2[(\lambda_2-\sigma_{11})\varsigma_{13}-\sigma_{12}\varsigma_{23}]\\&-\sigma_{12}(\sigma_{11}+1)[(\lambda_2-\sigma_{11})\varsigma_{14}-\sigma_{12}\varsigma_{24}]+(\sigma_{11}+1)^2[(\lambda_2-\sigma_{11})\varsigma_{15}-\sigma_{12}\varsigma_{25}]\},\\ \phi_4=&\frac{\sigma_2}{\sigma_{12}(\lambda_2+1)}\{\sigma_{12}[(\lambda_2-\sigma_{11})\varsigma_{11}-\sigma_{12}\varsigma_{21}]+(\lambda_2-\sigma_{11})[(\lambda_2-\sigma_{11})\varsigma_{12}-\sigma_{12}\varsigma_{22}]\},\\ \phi_5=&\frac{\sigma_1}{\sigma_{12}(\lambda_2+1)}\{2\sigma_{12}^2[(\lambda_2-\sigma_{11})\sigma_{13}-\sigma_{12}\sigma_{23}]+\sigma_{12}(\lambda_2-2\sigma_{11}-1)[(\lambda_2-\sigma_{11})\sigma_{14}-\sigma_{12}\sigma_{24}]\\&-2(\lambda_2-\sigma_{11})(\sigma_{11}+1)[(\lambda_2-\sigma_{11})\sigma_{15}-\sigma_{12}\sigma_{25}]\}+\frac{1}{\sigma_{12}(\lambda_2+1)}\{\sigma_{12}^3[(\lambda_2-\sigma_{11})\sigma_{16}-\sigma_{12}\sigma_{26}]\\&-(\sigma_{11}+1)^3[(\lambda_2-\sigma_{11})\sigma_{19}-\sigma_{12}\sigma_{19}]\}.\end{aligned}$$

If the discriminatory quantities β_1 and β_2 are not zero, then system (1.2) will undergo a period-doubling bifurcation. The discriminatory quantities β_1 and β_2 are determined by the following formulae

$$\beta_1 = \left(2\tilde{\mathscr{F}}_{U_n\widetilde{\eta_a}} + \tilde{\mathscr{F}}_{\widetilde{\eta_a}}\tilde{\mathscr{F}}_{U_nU_n}\right)\Big|_{(0,0)} = 2h_2,$$
$$\beta_2 = \frac{1}{3}\tilde{\mathscr{F}}_{U_nU_nU_n} + \frac{1}{2}\left(\tilde{\mathscr{F}}_{U_nU_n}\right)^2\Bigg|_{(0,0)} = 2\phi_5 + 2\phi_1^2.$$

The above discussion is summarized in the following theorem.

Theorem 3.1. *If $\beta_1 \neq 0$ and $\beta_2 \neq 0$, then the system (1.2) experiences a period-dobling bifurcation at point $E^*(u^*, v^*)$ when h passes the critical point $h_{1,2}$. The last condition is equivalent to condition that η_a crosses the critical point $\eta_{a_{1,2}}$. If $\beta_2 > 0$, the period two points branching from the fixed point $E^*(u^*, v^*)$ are stable, which is called a supercritical period-doubling bifurcation. Conversely, if $\beta_2 < 0$, the period two points branching from the fixed point $E^*(u^*, v^*)$ are unstable, which is called a subcritical period-doubling bifurcation.*

3.2. Neimark-Sacker bifurcation. Next, the existence of a Neimark-Sacker bifurcation at $E^*(u^*, v^*)$ is analyzed. Take system (1.2) into account, where the parameters $(\alpha, r, \theta_0, p, q, m, k, b, \theta_1, c, d, h) \in N$ are arbitrary. By considering a small perturbation $\hat{\eta}_a$ where $|\hat{\eta}_a| \ll 1$ into system (1.2), we obtain

$$\begin{aligned} u_{n+1}(t) &= u_n + (\eta_a^* + \hat{\eta}_a)\left(\frac{ru_n}{1+\theta_0 v_n} - pu_n - qu_n^2 - \frac{mu_nv_n}{u_n+kv_n}\right), \\ v_{n+1}(t) &= v_n + (\eta_a^* + \hat{\eta}_a)\left(bv_n\left(\frac{v_n}{v_n+\theta_1} - \frac{v_n}{cu_n+d}\right)\right). \end{aligned} \tag{3.5}$$

It can be checked that the Jacobian matrix of system (3.5) at $E^*(u^*, v^*)$ has the following characteristic equation

$$\lambda^2(\hat{\eta}_a) + \mathscr{P}(\hat{\eta}_a)\lambda + \mathscr{Q}(\hat{\eta}_a) = 0,$$

where $\mathscr{P}(\hat{\eta}_a) = -2 - \zeta_a(\eta_a^* + \hat{\eta}_a)$ and $\mathscr{Q}(\hat{\eta}_a) = 1 + \zeta_a(\eta_a^* + \hat{\eta}_a) + \omega_a(\eta_a^* + \hat{\eta}_a)^2$.

According to the previous analysis, if $(\alpha, r, \theta_0, p, q, m, k, b, \theta_1, c, d, h) \in N$ and $\hat{\eta}_a = 0$, then the eigenvalues of the Jacobian matrix (2.1) at E^* are a pair of conjugate complex numbers λ and $\bar{\lambda}$ where $|\lambda| = |\bar{\lambda}| = 1$. As $\hat{\eta}_a$ changes in the vicinity of $\hat{\eta}_a = 0$ then the eigenvalues of (2.1) are

$$\lambda(\hat{\eta}_a), \bar{\lambda}(\hat{\eta}_a) = \frac{-\mathscr{P}(\hat{\eta}_a) \pm i\sqrt{4\mathscr{Q}(\hat{\eta}_a) - \mathscr{P}^2(\hat{\eta}_a)}}{2} = 1 + \frac{\zeta_a(\eta_a^* + \hat{\eta}_a)}{2} \pm \frac{i(\eta_a^* + \hat{\eta}_a)\sqrt{4\omega_a - \zeta_a^2}}{2}.$$

We can show that $|\lambda(\hat{\eta}_a), \bar{\lambda}(\hat{\eta}_a)| = (\mathscr{Q}(\hat{\eta}_a))^{\frac{1}{2}}$ and if $\frac{mu^*v^*}{(u+kv^*)^2} + \frac{2bv^*\theta_1+bv^{*2}}{(v^*+\theta_1)^2} < qu^* + \frac{2bv^*}{cu^*+d}$, then $\left.\frac{d|\lambda,\bar{\lambda}|}{d\hat{\eta}_a}\right|_{\hat{\eta}_a=0} = -\frac{\zeta_a}{2} > 0$.

For the Neimark-Sacker bifurcation to occur, it is required that when $\hat{\eta}_a = 0$, the eigenvalues must satisfy $\lambda^j, \bar{\lambda}^j \neq 1$ $(j = 1,2,3,4)$. This condition corresponds to $\mathscr{P}(0) \neq -2,0,1,2$. As the parameter $(\alpha, r, \theta_0, p, q, m, k, b, \theta_1, c, d, h) \in N$, it follows that $\mathscr{P}(0) \neq -2,2$. Thus, we only need that $\mathscr{P}(0) \neq 0,1$, which implies that $\frac{\zeta_a^2}{\omega_a} \neq 2,3$. By taking $x_n = u_n - u^*$ and $y_n = v_n - v^*$, we shift the fixed point $E^*(u^*,v^*)$ of system (3.5) into the origin $(0,0)$. Then, by using Taylor expansion, we obtain the following system

$$\begin{aligned} x_{n+1} =& \sigma_{11}x_n + \sigma_{12}y_n + \sigma_{13}x_n^2 + \sigma_{14}x_ny_n + \sigma_{15}y_n^2 + \sigma_{16}x_n^3 + \sigma_{17}x_n^2y_n \\ &+ \sigma_{18}x_ny_n^2 + \sigma_{19}y_n^3 + O((|x_n| + |y_n| + |\tilde{h}|)^4), \\ u_{n+1} =& \sigma_{21}x_n + \sigma_{22}y_n + \sigma_{23}x_n^2 + \sigma_{24}x_ny_n + \sigma_{25}y_n^2 + \sigma_{26}x_n^3 + \sigma_{27}x_n^2y_n \\ &+ \sigma_{28}x_ny_n^2 + \sigma_{29}y_n^3 + O((|x_n| + |y_n| + |\tilde{h}|)^4). \end{aligned} \tag{3.6}$$

The values of $\sigma_{11}, \sigma_{12}, \sigma_{13}, \sigma_{14}, \sigma_{15}, \sigma_{16}, \sigma_{17}, \sigma_{18}, \sigma_{19}, \sigma_{21}, \sigma_{22}, \sigma_{23}, \sigma_{24}, \sigma_{25}, \sigma_{26}, \sigma_{27}, \sigma_{28}$, and σ_{29}, are defined in (3.3).

Next, we consider the normal form of equation (3.6) when $\hat{\eta}_a = 0$. Let $\gamma = \kappa_1 - \sigma_{11}$. By applying the translation $\begin{bmatrix} x_n \\ y_n \end{bmatrix} = T_2 \begin{bmatrix} U_n \\ V_n \end{bmatrix}$, where $T_2 = \begin{bmatrix} \sigma_{12} & 0 \\ \gamma & -\kappa_2 \end{bmatrix}$, the equation (3.6) can be written as

$$\begin{bmatrix} U_{n+1} \\ V_{n+1} \end{bmatrix} = \begin{bmatrix} \kappa_1 & -\kappa_2 \\ \kappa_2 & \kappa_1 \end{bmatrix} \begin{bmatrix} U_n \\ V_n \end{bmatrix} + \begin{bmatrix} \tilde{f}(U_n,V_n) \\ \tilde{g}(U_n,V_n) \end{bmatrix}, \tag{3.7}$$

where

$$\begin{aligned} \tilde{f}(U_n,V_n) =& \frac{1}{\sigma_{12}}(\sigma_{13}x_n^2 + \sigma_{14}x_ny_n + \sigma_{15}y_n^2 + \sigma_{16}x_n^3 + \sigma_{17}x_n^2y_n + \sigma_{18}x_ny_n^2 + \sigma_{19}y_n^3 + O((|x_n| + |y_n|)^4), \\ \tilde{g}(U_n,V_n) =& \frac{1}{\sigma_{12}\kappa_2}\{[\gamma\sigma_{13} - \sigma_{12}\sigma_{23}]x_n^2 + [\gamma\sigma_{14} - \sigma_{12}\sigma_{24}]x_ny_n + [\gamma\sigma_{15} - \sigma_{12}\sigma_{25}]y_n^2 \\ &+ [\gamma\sigma_{16} - \sigma_{12}\sigma_{26}]x_n^3 + [\gamma\sigma_{17} - \sigma_{12}\sigma_{27}]x_n^2y_n + [\gamma\sigma_{18} - \sigma_{12}\sigma_{28}]x_ny_n^2 \\ &+ [\gamma\sigma_{19} - \sigma_{12}\sigma_{29}]y_n^3 + O((|x_n| + |y_n|)^4)\}, \end{aligned}$$

with $x_n = \sigma_{12}U_n$ and $y_n = \gamma U_n - \kappa_2 V_n$. From equation (3.7), we can calculate that

$$\tilde{f}_{U_n,U_n} = \frac{2}{\sigma_{12}}[\sigma_{12}^2\sigma_{13} + \sigma_{14}\sigma_{12}\gamma + \sigma_{15}\gamma^2], \quad \tilde{f}_{U_n,V_n} = -\frac{1}{\sigma_{12}}[\kappa_2\sigma_{12}\sigma_{14} + 2\kappa_2\gamma\sigma_{15}],$$

$$\tilde{f}_{V_n,V_n} = \frac{2\kappa_2^2\sigma_{15}}{\sigma_{12}}, \quad \tilde{f}_{U_n,U_n,U_n} = \frac{6}{\sigma_{12}}[\sigma_{16}\sigma_{12}^3 + \sigma_{17}\sigma_{12}^2\gamma + \sigma_{18}\sigma_{12}\gamma^2 + \sigma_{19}\gamma^3],$$

$$\tilde{f}_{U_n,U_n,V_n} = -\frac{2}{\sigma_{12}}[\kappa_2\sigma_{17}\sigma_{12}^2 + 2\kappa_2\sigma_{18}\sigma_{12}\gamma + 3\kappa_2\sigma_{19}\gamma^2], \quad \tilde{f}_{U_n,V_n,V_n} = \frac{2\kappa_2^2}{\sigma_{12}}[\sigma_{18}\sigma_{12} + 3\kappa_2\sigma_{19}\gamma],$$

$$\tilde{f}_{V_n,V_n,V_n} = -\frac{6\kappa_2^3\sigma_{19}}{\sigma_{12}}, \quad \tilde{g}_{U_n,U_n} = \frac{2}{\sigma_{12}}(\sigma_{12}^2[\gamma\sigma_{13} - \sigma_{12}\sigma_{23}] + \sigma_{12}\gamma[\gamma\sigma_{14} - \sigma_{12}\sigma_{24}] + \gamma^2[\gamma\sigma_{15} - \sigma_{12}\sigma_{25}]),$$

$$\tilde{g}_{U_n,V_n} = -\frac{1}{\sigma_{12}}(\sigma_{12}[\gamma\sigma_{14} - \sigma_{12}\sigma_{24}] + 2\gamma[\gamma\sigma_{15} - \sigma_{12}\sigma_{25}]), \quad \tilde{g}_{V_n,V_n} = \frac{2\kappa_1}{\sigma_{12}}[\gamma\sigma_{15} - \sigma_{12}\sigma_{25}],$$

$$\tilde{g}_{U_n,U_n,U_n} = \frac{6}{\sigma_{12}\kappa_2}(\sigma_{12}^3[\gamma\sigma_{16}] + \sigma_{12}^2(\kappa_1 - \sigma_{11})[\gamma\sigma_{17} - \sigma_{12}\sigma_{27}] + \sigma_{12}\gamma^2[\gamma\sigma_{18} - \sigma_{12}\sigma_{28}]$$
$$+ \gamma^3[\gamma\sigma_{19} - \sigma_{12}\sigma_{29}]),$$

$$\tilde{g}_{U_n,U_n,V_n} = -\frac{2}{\sigma_{12}}(\sigma_{12}^2[\gamma\sigma_{17} - \sigma_{12}\sigma_{27}] + 2\sigma_{12}\gamma[\gamma\sigma_{18} - \sigma_{12}\sigma_{28}] + 3\gamma^2[\gamma\sigma_{19} - \sigma_{12}\sigma_{29}]),$$

$$\tilde{g}_{U_n,V_n,V_n} = \frac{2\kappa_2}{\sigma_{12}}(\sigma_{12}[\gamma\sigma_{18} - \sigma_{12}\sigma_{28}] + 3\gamma[\gamma\sigma_{19} - \sigma_{12}\sigma_{29}]), \quad \tilde{g}_{V_n,V_n,V_n} = -\frac{6\kappa_2^2}{\sigma_{12}}[\gamma\sigma_{19} - \sigma_{12}\sigma_{29}].$$

System (1.2) undergoes a Neimark-Sacker bifurcation if the following condition is satisfied

$$\Omega = -Re\left[\frac{(1-2\lambda)\bar{\lambda}^2}{1-\lambda}\xi_{11}\xi_{20}\right] - \frac{1}{2}|\xi_{11}|^2 - |\xi_{02}|^2 + Re(\bar{\lambda}\xi_{21}) \neq 0,$$

where

$$\xi_{20} = \frac{1}{8}[(\tilde{f}_{U_nU_n} - \tilde{f}_{V_nV_n} + 2\tilde{g}_{U_nV_n}) + i(\tilde{g}_{U_nU_n} - \tilde{g}_{V_nV_n} - 2\tilde{f}_{U_nV_n})],$$
$$\xi_{11} = \frac{1}{4}[(\tilde{f}_{U_nU_n} + \tilde{f}_{V_nV_n}) + i(\tilde{g}_{U_nU_n} + \tilde{g}_{V_nV_n})],$$
$$\xi_{02} = \frac{1}{8}[(\tilde{f}_{U_nU_n} - \tilde{f}_{V_nV_n} - 2\tilde{g}_{U_nV_n}) + i(\tilde{g}_{U_nU_n} - \tilde{g}_{V_nV_n} + 2\tilde{f}_{U_nV_n})],$$
$$\xi_{21} = \frac{1}{16}\left[(\tilde{f}_{U_nU_nU_n} + \tilde{f}_{U_nV_nV_n} + \tilde{g}_{U_nU_nV_n} + \tilde{g}_{V_nV_nV_n}) + i(\tilde{g}_{U_nU_nU_n} + \tilde{g}_{U_nV_nV_n}\right.$$
$$\left. - \tilde{f}_{U_nV_nV_n} - \tilde{f}_{V_nV_nV_n})\right].$$

Hence, according to the Neimark-Sacker bifurcation conditions in [44], the following theorem is obtained.

Theorem 3.2. *If* $\frac{mu^*v^*}{(u+kv^*)^2} + \frac{2bv^*\theta_1 + bv^{*2}}{(v^*+\theta_1)^2} < qu^* + \frac{2bv^*}{cu^*+d}$, $\frac{\zeta_a^2}{\omega_a} \neq 2$ *or* 3, *and* $\Omega \neq 0$, *then the system (1.2) experiences a Neimark-Sacker bifurcation at the point* $E^*(u^*, v^*)$ *when h passes the critical* *point h^*. The last requirement is the same as the conditionthat η_a passes its critical point η_a^*. If $\Omega < 0$, the mapping experiences a supercritical Neimark-Sacker bifurcation, whereas if $\Omega > 0$, the mapping experiences a subcritical Neimark-Sacker bifurcation.*

4. NUMERICAL SIMULATIONS

In this section, we perform numerical simulations for demonstrating the prior analytical finding and show the occurrences of period-doubling bifurcation and Neimark-Sacker bifurcation. There is no need to develop new computations method to solve our model, because our model is discrete and the iterative expressions are already provided. First, we take the values of parameters: $p = 0.239$, $q = 0.1$, $m = 0.904$, $b = 0.487$, $r = 2.68$, $c = 0.075$, $\theta_0 = 0.126$, $d = 0.583$, $\theta_1 = 0.583$, $k = 0.4$, $\alpha = 0.9$, and initial value $u(0) = 19.5$, $v(0) = 1.46$. For this case, system (1.2) has interior fixed point $E^*(19.5692, 1.4677)$, $\omega_a = 0.5762 > 0$, $\zeta_a^2 - 4\omega_a = 2.2853 > 0$, and $h_1 = 1.0588$. Thus, $(\alpha, r, \theta_0, p, q, m, k, b, \theta_1, c, d, h) \in P_1$. Theorem 2.4 states that the fixed point $E^*(19.5692, 1.4677)$ is a sink for $h < h_1$ and loses its stability at $h = h_1$. We also get $\beta_1 = -3.6542 \neq 0$, and $\beta_2 = 0.63196 \neq 0$. So, based on the Theorem 3.1, the system (1.2) undergoes a period-doubling bifurcation around $E^*(19.5692, 1.4677)$ and the bifurcation point is $h = h_1$. Furthermore, $\beta_2 > 0$ indicates the stability of the period-2 points (supercritical). This phenomenon is shown in the bifurcation diagram in Figure 1 (a) and (b), and the related maximum Lyapunov exponent (MLE) is presented in Figure 1 (c). It is seen clearly that if $h < h_1$, then $E^*(19.5692, 1.4677)$ is stable. If $h > h_1$, then the period-2 points remains stable and cascading period doubling appears. We can observed that there is a range of h values such that the system (1.2) experiences chaotic dynamics. The emergence of chaotic behavior is characterized by the presence of a positive MLE in several h ranges shown in Figure 1 (a). In Figure 2, the time series system (1.2) are given, which corresponds to Figure 1.

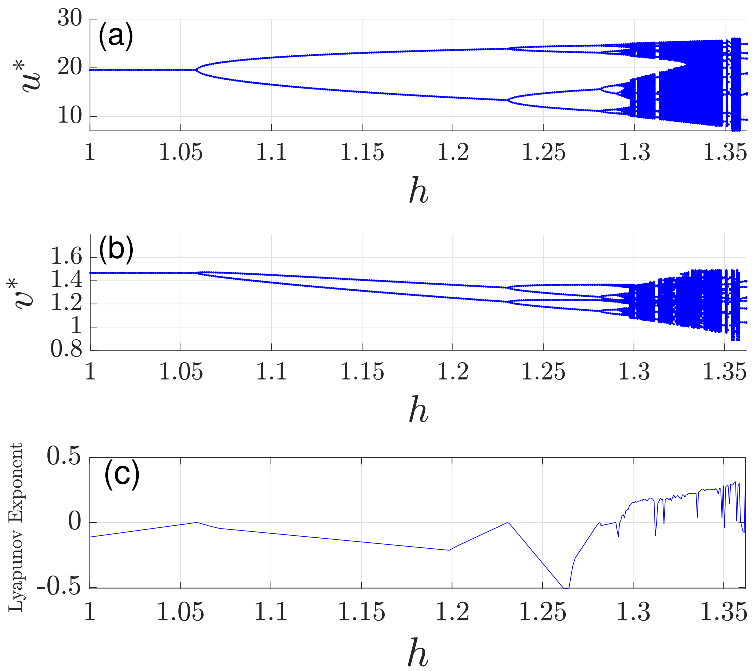

FIGURE 1. (a-b) Bifurcation diagram and (c) MLE of system (1.2) with $q = 0.1$, $b = 0.487$, $c = 0.075$, $\theta_0 = 0.126$.

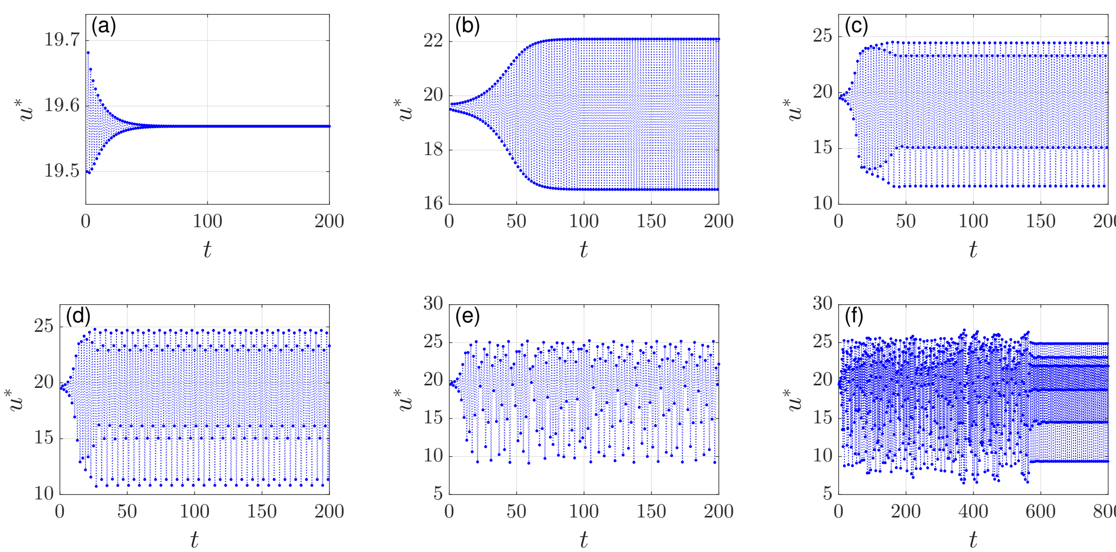

FIGURE 2. Time series solution of system (1.2) with $q = 0.1$, $b = 0.487$, $c = 0.075$, $\theta_0 = 0.126$ and (a) $h = 1.01$; (b) $h = 1.1$; (c) $h = 1.26$; (d) $h = 1.285$; (e) $h = 1.33$; (f) $h = 1.36$.

For the second simulation, we take $q = 0.047$, $b = 0.8$, $c = 0.943$, and $\theta_0 = 0.826$; while other parameters are the same as in the first simulation. System (1.2) with these parameters has interior fixed point of system (1.2) $E^*(2.2809, 2.1509)$. In this case, we also have $\omega_a = 0.3589 > 0$, $\zeta_a^2 - 4\omega_a = -1.4122 < 0$, and $h^* = 0.3712$. Hence, $(\alpha, r, \theta_0, p, q, m, k, b, \theta_1, c, d, h) \in N$. According to Theorem 2.4, $E^*(2.2809, 2.1509)$ is a sink when $h < h^*$ and loses stability when $h = h^*$. Morever, we can also check that $\lambda, \bar{\lambda} = 0.9674 \pm 0.2532i$ where $|\lambda(0), \bar{\lambda}(0)| = 1$,

$$\frac{mu^*v^*}{(u+kv^*)^2} + \frac{2bv^*\theta_1 + bv^{*^2}}{(v^*+\theta_1)^2} = 1.2131 < qu^* + \frac{2bv^*}{cu^*+d} = 1.366, \qquad \frac{\zeta_a^2}{\omega_a} = 0.0652 \neq 2, 3,$$

and $\Omega = -0.002995 < 0$. Therefore, Theorem 3.2 states that the system (1.2) experiences a supercritical Neimark-Sacker bifurcation around the fixed point $E^*(2.2809, 2.1509)$ at $h = h^*$. This phenomenon is clearly seen in the bifurcation diagrams and the MLE shown in Figure 3. The associated phase portraits of the system (1.2) are exhibited in Figure 4. We see in Figures 3 and 4 that the solution approaches a closed periodic orbit after h passes h^*. However, we also identify that the MLE has positive values at some intervals, which indicate the occurrence of chaotic behavior. This chaotic behavior is also shown in Figure 4 (e-f).

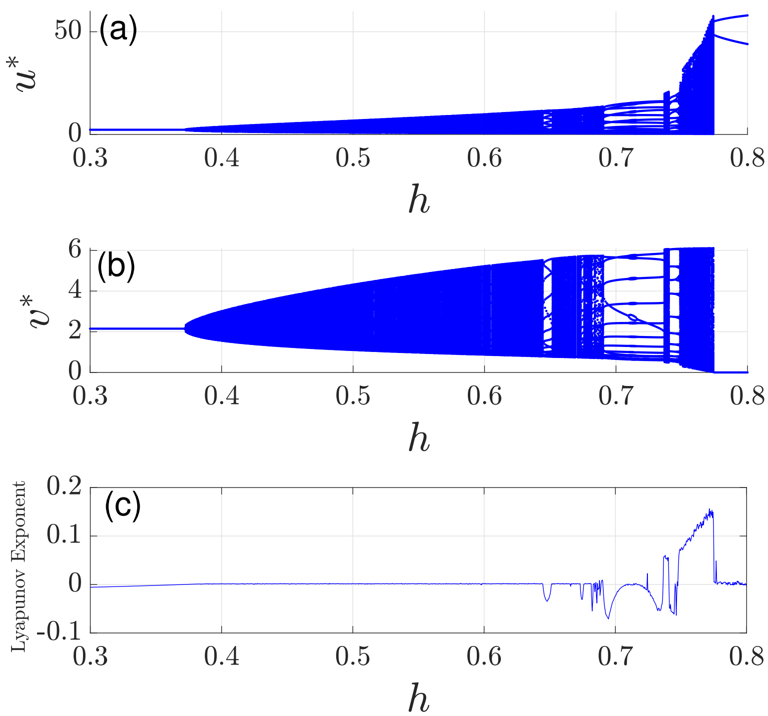

FIGURE 3. (a-b) Bifurcation diagram and (c) MLE of the system (1.2) with $q = 0.047$, $b = 0.8$, $c = 0.943$, $\theta_0 = 0.826$.

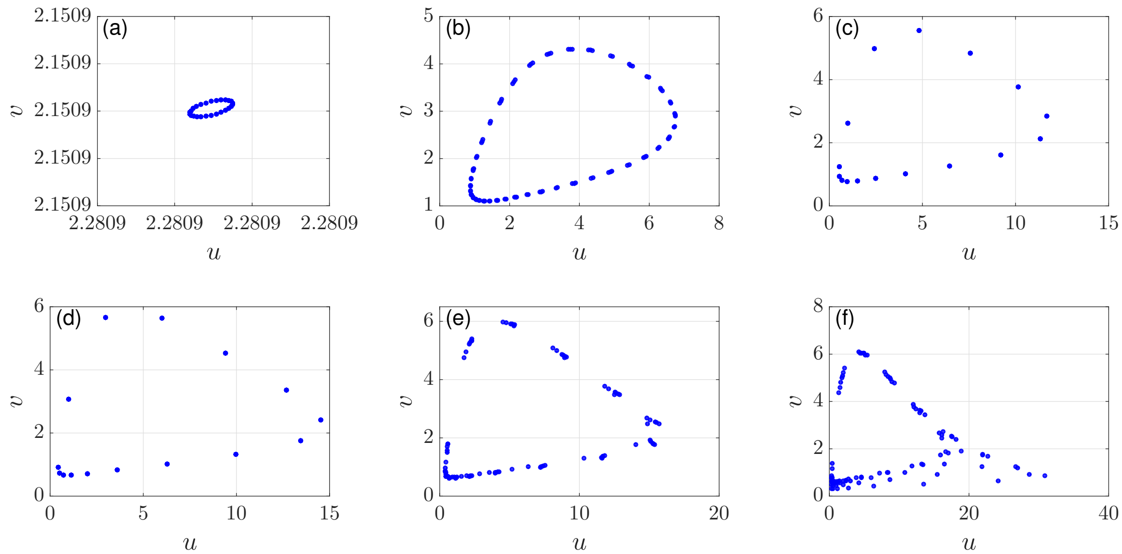

FIGURE 4. Phase portraits of system (1.2) with $q = 0.047$, $b = 0.8$, $c = 0.943$, $\theta_0 = 0.826$, and (a) $h = 0.35$; (b) $h = 0.5$; (c) $h = 0.65$; (d) $h = 0.7$; (e) $h = 0.738$; (f) $h = 0.76$.

5. CONCLUSION

The fractional-order Leslie-Gower model with discrete–time has been obtained using the PWCA method. It has been shown that this proposed discrete–time model has four fixed points: the extinction point of both populations, the extinction point of the predator, the extinction point of the prey, and the interior fixed point. The local stability of all fixed points has been thoroughly analyzed, demonstrating that it depends on both the model's parameters and the numerical integration time–step (h). We provide analytical proof that the proposed discrete–time model can undergo both period-doubling bifurcation and Neimark-Sacker bifurcation. Our numerical simulations validate this dynamic behavior. Additionally, our numerical simulations demonstrate that this discrete–time model can experience chaotic dynamics for certain parameter values. Thus, the discrete-time model presented reveals more intricate dynamics than those of the continuous version.

ACKNOWLEDGEMENTS

This research is funded by Faculty of Mathematics and Natural Science (FMIPA) through Public Funds DPA (Dokumen Pelaksanaan Anggaran) Perguruan Tinggi Negeri Berbadan Hukum

(PTNBH), University of Brawijaya and based on FMIPA Professor Grant, with contract number: 02172.18/UN10.F0901/B/KS/2024, dated July 12, 2024.

Conflict of Interests

The authors declare that there is no conflict of interests.

References

[1] D. Maknun, Ekologi: Populasi, Komunitas, Ekosistem Mewujudkan Kampus Hijau, Asri, Islami, dan Ilmiah, Nurjati Press, Cirebon, 2017.

[2] S.S. Mader, A. Baldwin, Biology, McGraw-Hill Higher Education, New York, 2010.

[3] A.J. Lotka, Elements of Mathematical Biology, Dover, New York, 1956.

[4] V. Volterra, Variazioni e Fluttuazioni del Numero d'Individui in Specie Animali Conviventi, in: Memoria del Socio Vito Volterra, Societá Anonima Tipografica "Leonardo da Vinci, Città di Castello, 1926.

[5] P.H. Leslie, J.C. Gower, The Properties of a Stochastic Model for Two Competing Species, Biometrika 45 (1958), 316–330. https://doi.org/10.1093/biomet/45.3-4.316.

[6] M.A. Aziz-Alaoui, M. Daher Okiye, Boundedness and Global Stability for a Predator-Prey Model with Modified Leslie-Gower and Holling-Type II Schemes, Appl. Math. Lett. 16 (2003), 1069–1075. https://doi.org/10.1016/S0893-9659(03)90096-6.

[7] G.Q. Sun, Mathematical Modeling of Population Dynamics with Allee Effect, Nonlinear Dyn. 85 (2016), 1–12. https://doi.org/10.1007/s11071-016-2671-y.

[8] P. Feng, Y. Kang, Dynamics of a Modified Leslie–Gower Model with Double Allee Effects, Nonlinear Dyn. 80 (2015), 1051–1062. https://doi.org/10.1007/s11071-015-1927-2.

[9] D. Indrajaya, A. Suryanto, A.R. Alghofari, Dynamics of Modified Leslie-Gower Predator-Prey Model with Beddington-DeAngelis Functional Response and Additive Allee Effect, Int. J. Ecol. Dev. 31 (2016), 60–71.

[10] L. Li, Z. Hou, Y. Mao, Dynamical Transition and Bifurcation of a Diffusive Predator–Prey Model with an Allee Effect on Prey, Commun. Nonlinear Sci. Numer. Simul. 126 (2023), 107433. https://doi.org/10.1016/j.cnsns.2023.107433.

[11] E. Rahmi, I. Darti, A. Suryanto, Trisilowati, H.S. Panigoro, Stability Analysis of a Fractional-Order Leslie-Gower Model with Allee Effect in Predator, J. Phys.: Conf. Ser. 1821 (2021), 012051. https://doi.org/10.1088/1742-6596/1821/1/012051.

[12] L.Y. Ning, X.F. Luo, B.L. Li, et al. An Effective Allee Effect May Induce the Survival of Low-Density Predator, Results Phys. 53 (2023), 106926. https://doi.org/10.1016/j.rinp.2023.106926.

[13] R.J. Taylor, Predation, Springer, Dordrecht, 1984. https://doi.org/10.1007/978-94-009-5554-7.

[14] S.L. Lima, L.M. Dill, Behavioral Decisions Made under the Risk of Predation: A Review and Prospectus, Canadian J. Zool. 68 (1990), 619–640. https://doi.org/10.1139/z90-092.

[15] S.L. Lima, Nonlethal Effects in the Ecology of Predator-Prey Interactions: What Are the Ecological Effects of Anti-Predator Decision-Making?, BioScience 48 (1998), 25–34. https://doi.org/10.2307/1313225.

[16] W. Cresswell, Predation in Bird Populations, J. Ornithol. 152 (2011), 251–263. https://doi.org/10.1007/s10336-010-0638-1.

[17] L.Y. Zanette, A.F. White, M.C. Allen, M. Clinchy, Perceived Predation Risk Reduces the Number of Offspring Songbirds Produce per Year, Science 334 (2011), 1398–1401. https://doi.org/10.1126/science.1210908.

[18] X. Wang, L. Zanette, X. Zou, Modelling the Fear Effect in Predator–Prey Interactions, J. Math. Biol. 73 (2016), 1179–1204. https://doi.org/10.1007/s00285-016-0989-1.

[19] H. Zhang, Y. Cai, S. Fu, W. Wang, Impact of the Fear Effect in a Prey-Predator Model Incorporating a Prey Refuge, Appl. Math. Comput. 356 (2019), 328–337. https://doi.org/10.1016/j.amc.2019.03.034.

[20] A.S. Purnomo, I. Darti, A. Suryanto, et al. Fear Effect on a Modified Leslie-Gower Predator-Prey Model with Disease Transmission in Prey Population, Eng. Lett. 31 (2023), 33.

[21] J. Chen, Y. Chen, Z. Zhu, F. Chen, Stability and Bifurcation of a Discrete Predator-Prey System with Allee Effect and Other Food Resource for the Predators, J. Appl. Math. Comput. 69 (2023), 529–548. https://doi.org/10.1007/s12190-022-01764-5.

[22] Y. Xue, Impact of Both-Density-Dependent Fear Effect in a Leslie-Gower Predator-Prey Model with Beddington-DeAngelis Functional Response, Chaos Solitons Fractals 185 (2024), 115055. https://doi.org/10.1016/j.chaos.2024.115055.

[23] Y. Chatibi, E.H. El Kinani, A. Ouhadan, Variational Calculus Involving Nonlocal Fractional Derivative with Mittag–Leffler Kernel, Chaos Solitons Fractals 118 (2019), 117–121. https://doi.org/10.1016/j.chaos.2018.11.017.

[24] Y. Yan, C. Kou, Stability Analysis for a Fractional Differential Model of HIV Infection of CD4+ T-Cells with Time Delay, Math. Comput. Simul. 82 (2012), 1572–1585. https://doi.org/10.1016/j.matcom.2012.01.004.

[25] H.A.A. El-Saka, Backward Bifurcations in Fractional-Order Vaccination Models, J. Egypt. Math. Soc. 23 (2015), 49–55. https://doi.org/10.1016/j.joems.2014.02.012.

[26] S. Mondal, A. Lahiri, N. Bairagi, Analysis of a Fractional Order Eco-epidemiological Model with Prey Infection and Type 2 Functional Response, Math. Methods Appl. Sci. 40 (2017), 6776–6789. https://doi.org/10.1002/mma.4490.

[27] R.P. Chauhan, R. Singh, A. Kumar, N.K. Thakur, Role of Prey Refuge and Fear Level in Fractional Prey–Predator Model with Anti-Predator, J. Comput. Sci. 81 (2024), 102385. https://doi.org/10.1016/j.jocs.2024.102385.

[28] A. Suryanto, I. Darti, H.S. Panigoro, et al. A Fractional-Order Predator–Prey Model with Ratio-Dependent Functional Response and Linear Harvesting, Mathematics 7 (2019), 1100. https://doi.org/10.3390/math7111100.

[29] H.S. Panigoro, E. Rahmi, A. Suryanto, et al. A Fractional Order Predator–Prey Model with Strong Allee Effect and Michaelis–Menten Type of Predator Harvesting, AIP Conf. Proc. 2498 (2022), 020018. https://doi.org/10.1063/5.0082684.

[30] M. Rayungsari, A. Suryanto, W.M. Kusumawinahyu, I. Darti, Dynamics Analysis of a Predator–Prey Fractional-Order Model Incorporating Predator Cannibalism and Refuge, Front. Appl. Math. Stat. 9 (2023), 1122330. https://doi.org/10.3389/fams.2023.1122330.

[31] P.K. Santra, G.S. Mahapatra, Dynamics of a Fractional-Order Prey-Predator Reserve Biological System Incorporating Fear Effect and Mixed Functional Response, Brazil. J. Phys. 54 (2024), 14. https://doi.org/10.1007/s13538-023-01397-4.

[32] G. Ranjith Kumar, K. Ramesh, A. Khan, et al. Dynamical Study of Fractional Order Leslie-Gower Model of Predator-Prey with Fear, Allee Effect, and Inter-Species Rivalry, Results Control Optim. 14 (2024), 100403. https://doi.org/10.1016/j.rico.2024.100403.

[33] I. Podlubny, Fractional Differential Equations, Academic Press, San Diego, 1999.

[34] R. Satriyantara, A. Suryanto, N. Hidayat, Numerical Solution of a Fractional-Order Predator-Prey Model With Prey Refuge and Additional Food for Predator, J. Exper. Life Sci. 8 (2018), 66–70.

[35] A. Singh, P. Deolia, Dynamical Analysis and Chaos Control in Discrete-Time Prey-Predator Model, Commun. Nonlinear Sci. Numer. Simul. 90 (2020), 105313. https://doi.org/10.1016/j.cnsns.2020.105313.

[36] S. Al-Nassir, Dynamic Analysis of a Harvested Fractional-Order Biological System with Its Discretization, Chaos Solitons Fractals 152 (2021), 111308. https://doi.org/10.1016/j.chaos.2021.111308.

[37] Md.J. Uddin, S.Md.S. Rana, S. Işık, F. Kangalgil, On the Qualitative Study of a Discrete Fractional Order Prey–Predator Model with the Effects of Harvesting on Predator Population, Chaos Solitons Fractals 175 (2023), 113932. https://doi.org/10.1016/j.chaos.2023.113932.

[38] Md.J. Uddin, S.Md. Sohel Rana, Qualitative Analysis of the Discretization of a Continuous Fractional Order Prey-Predator Model with the Effects of Harvesting and Immigration in the Population, Complexity 2024 (2024), 8855142. https://doi.org/10.1155/2024/8855142.

[39] A. Suryanto, A Dynamically Consistent Nonstandard Numerical Scheme for Epidemic Model With Saturated Incidence Rate, Int. J. Math. Comput. 13 (2011), 112–123.

[40] H.N. Agiza, E.M. Elabbasy, H. El-Metwally, et al. Chaotic Dynamics of a Discrete Prey-Predator Model With Holling Type II, Nonlinear Anal.: Real World Appl. 10 (2009), 116–129. https://doi.org/10.1016/j.nonrwa.2007.08.029.

[41] Q. Din, Complexity and Chaos Control in a Discrete-Time Prey-Predator Model, Commun. Nonlinear Sci. Numer. Simul. 49 (2017), 113–134. https://doi.org/10.1016/j.cnsns.2017.01.025.

[42] Y. Cai, C. Zhao, W. Wang, J. Wang, Dynamics of a Leslie–Gower Predator–Prey Model with Additive Allee Effect, Appl. Math. Model. 39 (2015), 2092–2106. https://doi.org/10.1016/j.apm.2014.09.038.

[43] S.N. Elaydi, Discrete Chaos: With Applications in Science and Engineering, Chapman and Hall/CRC, 2007. https://doi.org/10.1201/9781420011043.
S.N. Elaydi, Discrete Chaos: With Applications in Science and Engineering (2nd ed.), Chapman and Hall/CRC, New York, 2007. https://doi.org/10.1201/9781420011043.

[44] J. Guckenheimer, P. Holmes, Nonlinear Oscillations, Dynamical Systems, and Bifurcations of Vector Fields, Springer, New York, 1983. https://doi.org/10.1007/978-1-4612-1140-2.